IV International Conference on Computational Methods for Coupled Problems in Science and Engineering
COUPLED PROBLEMS 2011
M. Papadrakakis, E. Oñate and B. Schrefler (Eds)

MIXING SNAPSHOTS AND FAST TIME INTEGRATION OF PDEs

MARÍA-LUISA RAPÚN†, FILIPPO TERRAGNI† AND JOSÉ M. VEGA†

† Dpto. Fundamentos Matemáticos, E.T.S.I. Aeronáuticos
Universidad Politécnica de Madrid
Plaza Cardenal Cisneros 3, 28040 Madrid, Spain

Key words: Reduced Order Models, Proper Orthogonal Decomposition, Galerkin Projection, Partial Differential Equations

Abstract. *A local proper orthogonal decomposition (POD) plus Galerkin projection method was recently developed to accelerate time dependent numerical solvers of PDEs. This method is based on the combined use of a numerical code (NC) and a Galerkin system (GS) in a sequence of interspersed time intervals, I_{NC} and I_{GS}, respectively. POD is performed on some sets of snapshots calculated by the numerical solver in the I_{NC} intervals. The governing equations are Galerkin projected onto the most energetic POD modes and the resulting GS is time integrated in the next I_{GS} interval. The major computational effort is associated with the snapshots calculation in the first I_{NC} interval, where the POD manifold needs to be completely constructed (it is only updated in subsequent I_{NC} intervals, which can thus be quite small). As the POD manifold depends only weakly on the particular values of the parameters of the problem, a suitable library can be constructed adapting the snapshots calculated in other runs to drastically reduce the size of the first I_{NC} interval and thus the involved computational cost. The strategy is successfully tested in (i) the one-dimensional complex Ginzburg-Landau equation, including the case in which it exhibits transient chaos, and (ii) the two-dimensional unsteady lid-driven cavity problem.*

1 INTRODUCTION

Reduced order models (ROMs) have become an increasingly active research field along the last twenty years. This is due to their interest in both understanding basic mechanisms of fluid systems [7, 15] and improving prediction and design in industrial processes [4, 11]. Concerning the latter, in mature sectors such as automotive and aeronautics, a trend is observed to promote the use of computational fluid dynamics (CFD) in aerodynamics design, intending to decrease the huge cost of wind tunnel tests. The main difficulty is that traditional CFD approaches (such as direct numerical simulation or turbulence models)

still require huge computational resources and CPU time, especially in multi-parameter problems. As a consequence, reducing computational effort of CFD solvers is becoming a crucial step to facilitate their industrial use.

Proper orthogonal decomposition (POD) combined with projection of the governing equations onto a POD manifold has been seen to produce ROMs of both steady [1, 10] and evolution problems [3, 12] which allow to drastically decrease computational cost. In evolution problems, these models consist in (i) identifying a low dimensional POD manifold that contains a good approximation of the relevant dynamics and (ii) using as reduced order model the Galerkin system (GS) obtained by projecting the governing equations onto this manifold. A basis of the POD manifold is constructed by the method of snapshots [17], which consists in applying POD methodology to a set of numerically calculated snapshots spanning a portion of the phase space of the dynamical system that contains all relevant orbits. Time integration of the GS turns out to involve a much smaller computational effort than time integration of the original system.

A major drawback is that the resulting GS may exhibit spurious dynamics in a somewhat unpredictable way. The reason for that is still controversial, but seems to be due to the non-invariance of the POD manifold under the true dynamics [14]. Thus, intended solutions to this difficulty somehow correct either the GS or the POD manifold in order to make the latter invariant [6, 16]. In all these cases, the GS is intended to approach the system dynamics in a particular attractor, which can be periodic, quasi-periodic, or chaotic, and it is not suitable to reproduce transient behaviors.

A somewhat different approach, called *local POD plus Galerkin projection* (LPOD+GP) method, was presented in [13] for one-dimensional parabolic equations and extended in [18] for two-dimensional fluid dynamics problems. In both works, the LPOD+GP method turned out to be both quite computationally efficient and robust, providing a good approximation of the considered dynamics (either transients or a given attractor), eliminating spurious behaviors. The main idea (see the sketch in Fig. 1) is to combine a numerical code (NC) and a GS in interspersed time intervals, I_{NC} and I_{GS}, respectively. Snapshots are computed by the NC in each I_{NC} interval and are used to either calculate (in the first I_{NC} interval) or update (in subsequent I_{NC} intervals) the relevant POD modes. The governing equations are then Galerkin projected onto the most energetic POD modes to obtain a GS that is integrated in the next I_{GS} interval. Of course, the key point of the method is to decide when each I_{GS} interval must be terminated because the GS approximation is no longer acceptable. This is accomplished by means of an a priori error estimate based on the amplitude of some additional higher order modes. In addition, a second GS that retains a few more modes than necessary is integrated and (in conjunction with the above mentioned a priori error estimate) provides a safe criterion for switching between I_{GS} and I_{NC} intervals, even in cases in which the involved dynamics are really complex.

Since the first I_{NC} interval is much longer than the remaining I_{NC} intervals and the GS is much computationally inexpensive than the NC, the crucial step to further improve the

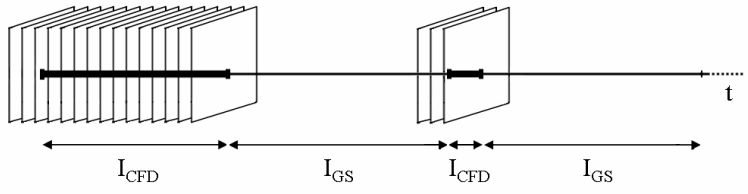

Figure 1: The local POD plus Galerkin projection method.

performance of the LPOD+GP method is to reduce the computational effort associated with the snapshots calculation in the first I_{NC} interval. A key observation is that the POD manifold depends only weakly on the particular values of the parameters of the problem. In this work we will show how a suitable *snapshots library* can be constructed from the POD manifolds calculated in other runs (for other parameter values). The use of this library allows for drastically reducing the size of the first I_{NC} interval and thus the involved computational cost. In other words, the library can be constructed using the POD modes obtained from a set of snapshots calculated by the NC for other parameter values (in, e.g., former applications of the LPOD+GP method). These POD modes may (possibly) not contain a good approximation of the true dynamics for the actual set of parameters, but they can be updated by adding a few snapshots for the true parameter values. The computation of these new snapshots only requires to use the NC in a small I_{NC} interval.

In order to explain and apply the introduced ideas, we will consider two test problems.

A. The *complex Ginzburg-Landau* (CGL) *equation*

$$\partial_t u = (1+\mathrm{i}\alpha)\partial_{xx}u + \mu u - (1+\mathrm{i}\beta)|u|^2 u, \quad \text{with } u = 0 \text{ at } x = 0, 1, \tag{1}$$

with initial condition $u(x,0) = \mathrm{i}\sin(2\pi x) + (1+\mathrm{i})\sin(3\pi x)$, which is a fairly simple equation that exhibits intrinsically complex dynamics [2]. The state variable u is complex and the parameters μ, α, and β are real. This equation exhibits the modulational instability if $\alpha\beta < 1$ and μ is large. Increasing μ beyond the modulational instability usually yields chaotic dynamics.

B. The *unsteady lid-driven cavity* (ULDC) *problem* [5, 8, 9], which describes the motion of a liquid in an enclosed cavity whose upper wall is moving back and forth. The governing equations are

$$\boldsymbol{\nabla}\cdot\boldsymbol{v} = 0, \qquad \partial_t \boldsymbol{v} + (\boldsymbol{v}\cdot\boldsymbol{\nabla})\boldsymbol{v} = -\boldsymbol{\nabla}p + \mathrm{Re}^{-1}\triangle\boldsymbol{v}, \tag{2}$$

in the spatial domain $0 < x < 1$, $0 < y < 1$, with boundary conditions

$$\boldsymbol{v} = \boldsymbol{0} \text{ at } x = 0, 1 \text{ and } y = 0, \qquad \boldsymbol{v} = \big(16\,h(t)x^2(1-x)^2, 0\big) \text{ at } y = 1. \tag{3}$$

Here, $\boldsymbol{v} = (v_x, v_y)$ and p are the dimensionless velocity and pressure, and the Reynolds number is defined as $\mathrm{Re} = u^* L/\nu$, where u^* is the maximum lid forcing (horizontal) velocity, L is the width of the cavity, and ν is the kinematic viscosity. The function h accounts for temporal oscillations (either periodic or quasi-periodic). Such time dependence of the driving velocity permits nontrivial dynamics at large time for moderate Reynolds number.

The remainder of the paper is organized as follows. The basic LPOD+GP method is briefly recalled and its improvement using POD modes libraries is developed in section 2, where notation is established. The results of the paper are presented and discussed in section 3. The paper ends with some concluding remarks, in section 4.

2 THE LOCAL POD PLUS GALERKIN PROJECTION METHOD

Let us consider a real or complex system of semilinear parabolic equations of the type

$$\boldsymbol{\mathcal{M}}\partial_t \boldsymbol{q} = \boldsymbol{\mathcal{L}}\boldsymbol{q} + \boldsymbol{f}(\boldsymbol{q}, t), \tag{4}$$

where $\boldsymbol{q}$ is a state vector, $\boldsymbol{\mathcal{M}}$ and $\boldsymbol{\mathcal{L}}$ are linear operators, with the highest order derivatives accounted for in $\boldsymbol{\mathcal{L}}$, and $\boldsymbol{f}$ is a nonlinear operator. In the I_{GS} intervals, $\boldsymbol{q}$ is approximated by a linear combination of POD modes $\boldsymbol{Q}_i$ as

$$\boldsymbol{q} \simeq \boldsymbol{q}^n_{\mathrm{GS}} = \sum_{i=1}^{n} A_i(t)\boldsymbol{Q}_i, \tag{5}$$

for certain amplitudes A_i [1]. Replacing (5) into (4) and projecting the resulting equations onto the POD modes, yields the following GS

$$\sum_{j=1}^{n} \mathcal{M}^{\mathrm{GS}}_{ij} \frac{dA_j}{dt} = \sum_{j=1}^{n} \mathcal{L}^{\mathrm{GS}}_{ij} A_j + f^{\mathrm{GS}}_i(A_1, \ldots, A_n, t), \tag{6}$$

where the matrices $\boldsymbol{\mathcal{M}}^{\mathrm{GS}}$ and $\boldsymbol{\mathcal{L}}^{\mathrm{GS}}$, and the nonlinear functions f^{GS}_i are defined as

$$\mathcal{M}^{\mathrm{GS}}_{ij} = \langle \boldsymbol{Q}_i, \boldsymbol{\mathcal{M}}\boldsymbol{Q}_j \rangle, \quad \mathcal{L}^{\mathrm{GS}}_{ij} = \langle \boldsymbol{Q}_i, \boldsymbol{\mathcal{L}}\boldsymbol{Q}_j \rangle, \quad f^{\mathrm{GS}}_i = \langle \boldsymbol{Q}_i, \boldsymbol{f}(\sum_{k=1}^{n} A_k \boldsymbol{Q}_k, t) \rangle. \tag{7}$$

POD and Galerkin projection are performed in terms of a suitable inner product $\langle \cdot, \cdot \rangle$. Computational efficiency of the LPOD+GP method is enhanced by using an inner product based on a limited number of discretization mesh points [13, 18]. Note that POD modes are orthonormal with respect to the considered inner product.

[1] When the boundary conditions are nonhomogeneous $\boldsymbol{q}$ is usually replaced by $\boldsymbol{q} - \boldsymbol{q}_0$ in the expansion (5), where $\boldsymbol{q}_0$ satisfies the nonhomogeneous boundary conditions.

In the first I_{NC} interval, POD modes are calculated from a set of N snapshots, namely N instantaneous distributions of $\boldsymbol{q}$. After truncation to $n \leq N$ modes, the relative root mean square error when reconstructing the N snapshots is given by

$$\mathrm{RRMSE}_n^N = \sqrt{\frac{\sum_{j=n+1}^{N}(\sigma_j)^2}{\sum_{j=1}^{N}(\sigma_j)^2}}, \tag{8}$$

where σ_j is the singular value associated with the mode $\boldsymbol{Q}_j$. This formula is used to select the number of retained modes. In subsequent I_{NC} intervals, the POD manifold is only updated by applying POD to the following set of vectors

$$\hat{\nu}_1\hat{\boldsymbol{Q}}_1, \ldots, \hat{\nu}_n\hat{\boldsymbol{Q}}_n, \nu_1\boldsymbol{Q}_1, \ldots, \nu_N\boldsymbol{Q}_N. \tag{9}$$

Here, $\hat{\boldsymbol{Q}}_1, \ldots, \hat{\boldsymbol{Q}}_n$ are the POD modes used in the last I_{GS} interval, while the weights $\hat{\nu}_1, \ldots, \hat{\nu}_n, \nu_1, \ldots, \nu_N$ are defined as

$$\hat{\nu}_j = \min\left\{\frac{\hat{\sigma}_j}{\sqrt{\sum_{k=1}^{n}(\hat{\sigma}_k)^2}}, \frac{\langle|A_j|\rangle}{\sqrt{\sum_{k=1}^{n}\langle|A_k|\rangle^2}}\right\}, \quad \nu_j = \frac{\sigma_j}{\sqrt{\sum_{k=1}^{N}(\sigma_k)^2}}, \tag{10}$$

where, for each j, $\hat{\sigma}_j$ is the singular value associated with $\hat{\boldsymbol{Q}}_j$ calculated in the last I_{NC} interval and $\langle|A_j|\rangle$ is the temporal mean value of $|A_j|$ in the last I_{GS} interval; $\boldsymbol{Q}_1, \ldots, \boldsymbol{Q}_N$ are the POD modes calculated from the new snapshots in the new I_{NC} interval, and $\sigma_1, \ldots, \sigma_N$ are the corresponding singular values. By defining the weights of old and new POD modes as in (10), we appropriately update the POD manifold avoiding its contamination and making it dependent on the local dynamics [13, 18].

The instantaneous, spatial, relative error associated with the Galerkin approximation (5) in each I_{GS} interval is measured by

$$\mathrm{E}^n = \|\boldsymbol{q} - \boldsymbol{q}^n_{\mathrm{GS}}\| \,/\, \|\boldsymbol{q}\|. \tag{11}$$

If E^{n_1} is sufficiently small for some $n_1 > n$, then the quantity

$$E_n^{n_1} = \sqrt{\frac{\sum_{j=n+1}^{n_1}(A_j)^2}{\sum_{j=1}^{n_1}(A_j)^2}} \tag{12}$$

is a good estimate of E^n [13, 18]. This error estimate is fairly standard and plays an essential role in the LPOD+GP method.

Now, the LPOD+GP method intends to approximate the solution of (4) within an error bound ε in each I_{GS} interval. This goal is achieved by retaining at the beginning of each I_{GS} interval a few more modes than necessary, which also provides an error estimate to monitor the error [13, 18]. The method also involves a second GS which allows to deal with highly unstable dynamics [13, 18].

2.1 The basic method

As developed in [13, 18], the basic LPOD+GP method proceeds as follows. A previous selection is made of the various parameters of the method appearing below, namely the RRMS error bound, ε, the constant K, the time interval between snapshots, δ_{snaps}, the number of snapshots in the first I_{NC} interval, and the minimum length of the I_{GS} intervals, $\delta_{GS,\min}$. The LPOD+GP method can then be summarized in four steps, as follows.

i. In the first I_{NC} interval, POD modes are calculated taking as snapshots the selected δ_{snaps}-equispaced portraits of $\boldsymbol{q}$. In the remaining I_{NC} intervals, POD modes are calculated from the modified snapshots defined in (9).

ii. Three numbers of modes, n, n_1, and n_2, are defined as the smallest integers satisfying $\text{RRMSE}_n^N < \varepsilon_1 = \varepsilon/K$, $\text{RRMSE}_{n_1}^N < \varepsilon_1/K$, $\text{RRMSE}_{n_2}^N < \varepsilon_1/K^2$, where the RRMSE is defined in terms of the singular values as in equation (8) and the parameter K needs to be calibrated (see [13, 18] and §2.2).

iii. Two GSs are constructed, retaining n_1 and n_2 modes, to calculate $\boldsymbol{q}_{\text{GS}}^{n_1} = \sum_{j=1}^{n_1} A_j \boldsymbol{Q}_j$ and $\tilde{\boldsymbol{q}}_{\text{GS}}^{n_2} = \sum_{j=1}^{n_2} \tilde{A}_j \boldsymbol{Q}_j$, respectively, taking as initial condition at $t = t_0 + \delta_{NC}$ the projections onto the POD manifolds of the NC solution calculated in step (i). Both GSs are integrated monitoring the error estimate $E_n^{n_1}$ defined in (12) and the following estimate of E^{n_1}, $\hat{E}_{n_1}^{n_2} = |\|\boldsymbol{q}_{\text{GS}}^n - \tilde{\boldsymbol{q}}_{\text{GS}}^{n_2}\|/\|\tilde{\boldsymbol{q}}_{\text{GS}}^{n_2}\| - E_n^{n_1}|$. Integration proceeds until the last value of t, t_1, such that

$$E_n^{n_1} \leq \varepsilon, \quad \hat{E}_{n_1}^{n_2} \leq \varepsilon_1. \tag{13}$$

The second restriction in (13) is used to impose consistency between the two GSs in connection with higher order modes. Now, there are two alternatives.

1. If the resulting value of $\delta_{GS} < \delta_{GS,\min}$, then a new value of δ_{NC} is defined as $\delta_{NC,\text{new}} = \min\{\delta_{NC,\text{estimated}}, 2\delta_{NC,\text{old}}\}$, where

$$\delta_{NC,\text{estimated}} = \delta_{NC,\text{old}} + \max\left\{\delta_{\text{snaps}}, \frac{\delta_{GS,\min} - \delta_{GS}}{\delta_{GS,\min}} \delta_{NC,\text{old}}\right\}.$$

   The NC solution is completed in the new part added to the I_{NC} interval and step (ii) is repeated.

2. Otherwise, the method proceeds to next step.

iv. If $t_1 < T$ (final value of t), then the value of $\boldsymbol{q}$ at t_2 reconstructed from the last Galerkin state with n_2 modes is taken as initial condition, and step (i) is repeated. Otherwise, the procedure ends.

The effectiveness of the LPOD+GP method can be measured in terms of the ratio of the total time span to the total length of the I_{NC} intervals, namely

$$\text{Theoretical Compression} = T/\sum \delta_{NC}. \tag{14}$$

The actual CPU compression factor may also be defined [18], which obviously depends on the CPU unit and the software used to construct the ROM.

As thoroughly shown in [13, 18], the method produces fairly good results (namely, the method provides the solution within the required precision, with large theoretical compression factors), which is due to the fact that the a priori error estimate defined above works quite well.

2.2 Improved method using weighted POD modes libraries

The POD modes library can be constructed in various ways, including:

- The POD manifold resulting from applying POD to a set of generic functions, such as Fourier and orthogonal polynomials, depending on the boundary conditions.
- The POD manifold resulting from other runs of the method for other parameter values. In this case, the weights of the POD modes are those appearing in the last I_{NC} interval, defined in eq.(10).
- Different libraries can be mixed up by just applying POD to the joint sets of modes, after appropriately weighting them as explained in the previous item.

Once the POD modes library is defined, it is used in the first I_{NC} interval as done in the basic method with the old POD manifold in subsequent I_{NC} intervals. In other words, the POD manifold in the first I_{NC} interval is calculated by applying POD to the set (9), where $\hat{\nu}_j \hat{\boldsymbol{Q}}_j$ are the weighted modes from the library, while $\nu_j \boldsymbol{Q}_j$ are as in eq.(9).

The idea is that the required number of snapshots, N, will be small provided that the POD modes library includes some of the directions in the required POD manifold. In fact, the selection of the library is not critical.

3 RESULTS

For illustration, the basic LPOD+GP method and its improvement described above are now applied to the two test problems introduced in §1.

3.1 The complex Ginzburg-Landau equation

In the CGL equation, the numerical solver results from discretizing the spatial derivatives with centered, second order finite differences, and integrating the resulting system of ODEs using Matlab ode15s, which is also used to time integrate the Galerkin system.

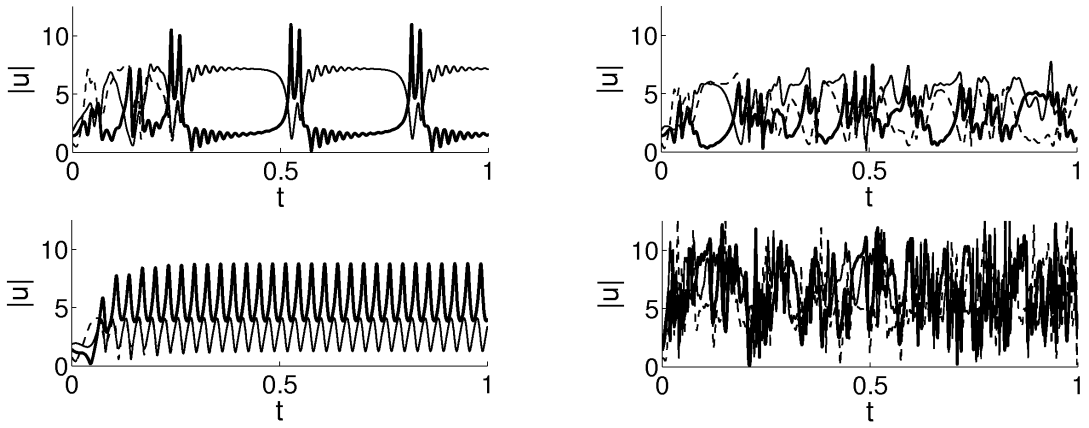

Figure 2: CGL equation: evolution at the points $x = 1/2$ (——), $x = 1/4$ (——), and $x = 3/4$ (– – –) in the test cases TC1 (top, left), TC2 (top, right), TC3 (bottom, left), and TC4 (bottom, right).

Four test cases are considered, which are defined for the following parameter values

$$(\mu, \alpha, \beta) = (95, -1.5, 12) \quad \text{(TC1)}, \quad (\mu, \alpha, \beta) = (85, -2, 19) \quad \text{(TC2)}, \tag{15}$$

$$(\mu, \alpha, \beta) = (65, -1.5, 10) \quad \text{(TC3)}, \quad (\mu, \alpha, \beta) = (180, -2, 15) \quad \text{(TC4)}. \tag{16}$$

These yield representative dynamics of the equation (see Fig.2) and will be used to construct POD modes libraries. The first two of them will also be used to check the performance of the method. Note that after a transient the system shows reflection symmetric relaxation oscillations in TC1 and even simpler oscillations in TC3, while TC2 and TC4 show representative, non-reflection symmetric chaotic dynamics.

The performance of the basic and improved versions of the method is illustrated in Fig.3, where the lengths of the interspersed I_{NC} and I_{GS} intervals is indicated in terms of the time steps required in each of them, both using the basic version of the method (labelled as LPOD+GP) and the improved version of the method, with various libraries, as indicated. The label L_F stands for the library resulting from applying POD to the set of Fourier modes $\sin(\ell\pi x)$, for $\ell = 1, \ldots, 50$, and the labels $L_{\text{TC}k}$, for $k = 1, \ldots, 4$, denote the last POD manifold resulting from the application of the basic LPOD+GP method to the test case TCk in the interval $0 \leq t \leq 1$; $L_F + L_{TC3}$ and $L_{TC1} + L_{TC3}$ denote the libraries resulting from mixing (as explained above) the two indicated libraries. The parameters of the method are $\varepsilon = 0.005$, $K = 100$, $\delta_{\text{snaps}} = 0.0005$, and $\delta_{GS,\text{min}} = 0.06$; the numbers of required POD modes are of the order of $(n, n_1, n_2) = (25, 30, 40)$ in both test cases TC1 and TC2. As a general comment, both the basic and the improved method work as well as the basic method did in [13].

Some remarks are now in order. Concerning the test case TC1 (left plots in Fig.3):

- The basic LPOD+GP method requires only two I_{NC} intervals, whose lengths are 403 and 1 time steps. The theoretical compression factor is 4.95.

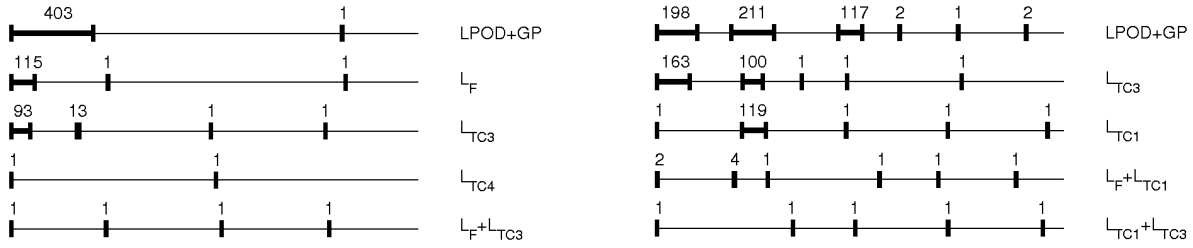

Figure 3: CGL equation: the I_{NC} (——) and I_{GS} (——) intervals in $0 \leq t \leq 1$ for the test cases TC1 (left) and TC2 (right). The number shown above each I_{NC} interval is the number of required time steps.

- Using both the generic library L_F and the customized library L_{TC3} produce similar results, namely they divide by 3.5 the length of the first I_{NC} interval (the new compression factor is 18.39). This is because the dynamics of the test case TC3 are much simpler than those of the test case that is simulated (see Fig.2).

- Using the library L_{TC4} produces optimal results since it reduces the length of the first I_{NC} interval to its minimum possible value, namely just one time step (the resulting compression factor is 1000). This is because the new library results from the test case TC4, which exhibits more complex dynamics than the dynamics that are being simulated. It is remarkable that the parameter values of the test cases TC1 and TC4 are quite different from each other (see eqs.(15)-(16)).

- If the (somewhat simple) libraries L_F and L_{TC3} are mixed up, the performance of the method is as optimal as when using the (more complex) library L_{TC4}. This seems to be due to the fact that each one of the libraries L_F and L_{TC3} spans a limited part of the phase space of the equation, but when these two libraries are mixed up, the resulting library spans a larger part of the phase space. The latter is in fact large enough as to allow for completing the POD manifold calculation with a slight updating in the first I_{NC} interval.

The last two remarks illustrate well the robustness of the method. The performance of the basic and improved LPOD+GP methods for the test case TC2 (right plots in Fig.3) exhibits similar trends. The main difference is that the dynamics of TC2 are more complex and the basic LPOD+GP method requires larger I_{NC} intervals. The improved method instead highly decreases the I_{NC} intervals, especially when the L_{TC1} and L_{TC3} libraries (both resulting from much simpler dynamics than the dynamics of TC2) are mixed up, which increases the compression factor from 3.76 to 400.

Finally, to further illustrate the robustness of the method, a random generation of the parameters of the CGL equation (1) in the intervals $\mu \in [50, 100]$, $\alpha \in [-2.5, -1.5]$, $\beta \in [10, 20]$ produced the values $(\mu, \alpha, \beta) = (81.87, -1.77, 15.45)$. In this case the method behaves as before: without libraries the compression factor is 3.01, while using the libraries

L_{TC3}, L_{TC1}, $L_F + L_{\mathrm{TC1}}$, and $L_{\mathrm{TC1}} + L_{\mathrm{TC3}}$ the compression factors are 8.24, 15.06, 333, and 400, respectively.

3.2 The unsteady lid-driven cavity problem for Re=100

The numerical solver for the ULDC problem (2)–(3) is a rough industrial-like code, which includes some artificial tricks to accelerate its performance. The Galerkin projection instead is based on the exact equations, discretized using a classical Crank-Nicolson scheme; see [18] for details. Five test cases are now considered to build up the POD modes libraries. These test cases are obtained using the following lid driving function h (appearing in the boundary condition (3)):

$$h = \sin(2\pi t/7)\cos(t/14) \quad \text{(TC1)}, \qquad h = \sin(\pi t/10)\cos(5t/4) \quad \text{(TC2)},$$
$$h = \sin(2t/\pi) + 0.5\cos t \quad \text{(TC3)}, \qquad h = \sin t \quad \text{(TC4)}, \qquad h = 1 \quad \text{(TC5)}.$$

Note that the first three of them are quasi-periodic, the fourth one is periodic, and the last one is steady. The initial condition is always the quiescent state, meaning that all of them exhibit unsteady behaviors, even under steady forcing.

The counterpart of Fig.3 is Fig.4. Note that the compression factors are now smaller, which is due to the nature of the numerical solver that is being used. Otherwise, the performance of the basic and improved LPOD+GP method exhibits the same trends as in the CGL equation. In particular:

- The libraries always shorten the length of the first I_{NC} interval, and this effect is stronger when the library results from a test case that exhibits more complex dynamics.
- Mixing libraries always produces a larger benefit than when each library is used alone. This is true even in cases in which the dynamics implicit in the libraries are simpler than the dynamics that are being simulated.
- The reduction of the first I_{NC} interval (which was already somewhat small as resulting from the basic LPOD+GP method) is only moderate, but the libraries also succeed in reducing the length of the subsequent I_{NC} intervals, thus improving the overall performance of the method.

4 CONCLUSIONS

A method based on POD modes libraries has been developed that highly improves the performance of the basic LPOD+GP method. The improvement has been illustrated and checked in two paradigmatic examples, namely the complex Ginzburg-Landau equation and the unsteady lid-driven cavity problem. The following remarks are in order:

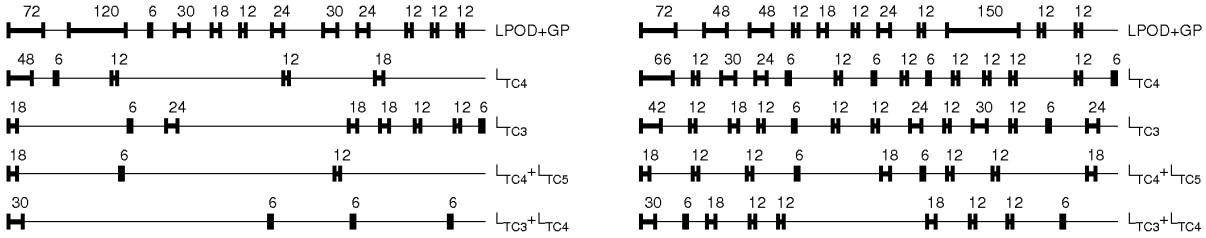

Figure 4: Counterpart of Fig.3 for the ULDC problem.

- The selection of the POD modes libraries is not critical. They can be constructed either out of a set of generic functions or using POD manifolds resulting from previous runs of the method for different parameter values. This is quite interesting envisaging applications in industrial environments, where solvers are usually run for a large amount of sets of parameter values.

- The libraries resulting from more complex dynamics than those that are being simulated usually work better than the libraries resulting from simpler dynamics.

- The combination of POD modes libraries usually produces much better results than when each library is used alone.

All these suggest that many parabolic equations and systems might exhibit a POD manifold that approximately contains (or almost contains) not only the attractors but also a significant part of the most relevant transient behaviors.

REFERENCES

[1] D. Alonso, A. Velazquez, and J. M. Vega, *A method to generate computationally efficient reduced order models*, Comput. Meth. Appl. Mech. Eng., 198 (2009), pp. 2683–2691.

[2] I. S. Aranson and L. Kramer, *The world of the complex Ginzburg-Landau equation*, Rev. Mod. Phys., 74 (2002), pp. 100–142.

[3] G. Berkooz, P. Holmes, and J. L. Lumley, *The proper orthogonal decomposition in the analysis of turbulent flows*, Annu. Rev. Fluid Mech., 25 (1993), pp. 539–575.

[4] K. Bizon, G. Continillo, L. Russo, and J. Smula, *On POD reduced models of tubular reactor with periodic regimes*, Comput. Chem. Eng., 32 (2008), pp. 1305–1315.

[5] W. Cazemier, R. W. C. P. Verstappen, and A. E. P. Veldman, *Proper orthogonal decomposition and low-dimensional models for driven cavity flows*, Phys. Fluids, 10 (1998), pp. 1685–1699.

[6] M. Couplet, C. Basdevant, and P. Sagaut, *Calibrated reduced-order POD-Galerkin system for fluid flow modelling*, J. Comput. Phys., 207 (2005), pp. 192–220.

[7] E. H. Dowell and K. C. Hall, *Modeling of fluid-structure interaction*, Annu. Rev. Fluid Mech., 33 (2001), pp. 445–490.

[8] P. W. Duck, *Oscillatory flow inside a square cavity*, J. Fluid Mech., 122 (1982), pp. 215–234.

[9] U. Ghia, K. N. Ghia, and C. T. Shin, *High-Re solutions for incompressible flow using the Navier-Stokes equations and a multigrid method*, J. Comput. Phys., 48 (1982), pp. 387–411.

[10] P. LeGresley and J. Alonso, *Investigation of non-linear projection for POD based reduced order models for Aerodynamics*, AAIA paper 2001-0926, Jan. 2001.

[11] T. Lieu, C. Farhat, and M. Lesoinne, *Reduced-order fluid/structure modeling of a complete aircraft configuration*, Comput. Meth. Appl. Mech. Eng., 195 (2006), pp. 5730–5742.

[12] D. J. Lucia, P. S. Beran, and W. A. Silva, *Reduced-order modelling: new approaches for computations physics*, Prog. Aeosp. Sci., 40 (2004), pp. 51–117.

[13] M. L. Rapún and J. M. Vega, *Reduced order models based on local POD plus Galerkin projection*, J. Comput. Phys., 229 (2010), pp. 3046–3063.

[14] D. Rempfer, *On low-dimensional Galerkin models for fluid flow*, Theor. Comput. Fluid Dyn., 14 (2000), pp. 75–88.

[15] D. Rempfer, *Low-dimensional modeling and numerical simulation of transition in simple shear flows*, Annu. Rev. Fluid Mech., 35 (2003), pp. 229–265.

[16] S. Sirisup, G. E. Karniadakis, D. Xiu, and I. G. Kevrekidis, *Equations-free/Galerkin-free POD assisted computation of incompressible flows*, J. Comput. Phys., 207 (2005), pp. 568–587.

[17] L. Sirovich, *Turbulence and the dynamics of coherent structures*, Q. Appl. Math., XLV (1987), pp. 561–590.

[18] F. Terragni, E. Valero, and J. M. Vega, *Local POD plus Galerkin projection in the unsteady lid-driven cavity problem*, preprint, 2010.